

The detection of organic polymers as contaminants in foodstuffs by means of the fluorescence decay of their auto fluorescence

Martin Versen^{a,*}, Maximilian Wohlschläger^a, Heinz Langhals^b, Christian Laforsch^c

^a Faculty of Engineering Sciences, Rosenheim Technical University of Applied Sciences, Hochschulstraße 1, Rosenheim 83024, Germany

^b LMU University of Munich, Department Chemistry, Butenandstr. 13, Munich D-81377, Germany

^c Animal Ecology I and BayCEER, University Bayreuth, Universitätsstraße 30, Bayreuth 95440, Germany

ARTICLE INFO

Keywords:

Fluorescence
Decay constant
Foodstuff
Imaging
Quality control
Organic polymers

ABSTRACT

Products such as food can become contaminated during their manufacture or afterwards. Depending on the type of substance causing the contamination, these contaminants can be harmful to health and difficult to detect by visible inspection. The suitability of fluorescence decay and FD-FLIM for the detection of plastics contamination in foodstuffs is demonstrated. Therefore, a procedure for the detection of contaminating organic polymers (plastics) in processed meat such as salami by means of the fluorescence decay time of auto fluorescence is described. The auto fluorescence of processed meat was found to decay according to first order with a typical time constant of about 2 ns, whereas the time constant of significant polymers for the processing of meat is generally appreciably higher (2.5 ns – 5.5 ns depending on the polymer). As a consequence, contaminating organic polymers can not only be globally detected by means of the fluorescence decay but also localised in two-dimensional imaging. The present study reports a high potential of FD-FLIM for rapidly identifying and differentiating different plastics on and in different foodstuffs. The method allows an improved quality control of foodstuffs.

1. Introduction

The development of technical organic polymers (plastics) was an essential improvement for the hygiene of foodstuff, where the necessary technology was developed for the generally recyclable plastic one-way packages; one can expect an increasing use of these materials. Moreover, plastics are lightweight, easily mouldable and exhibit favourable lubricating properties for dynamic components of machines. As a consequence, plastics are widely used in transport and processing of foodstuff (DIN Deutsches Institut für Normung e. V, 1994). However, there are also disadvantages of plastics because of possible unwanted contaminations of foodstuff such as processed meat; they are hardly detectable after grinding during processing because of the colour and structurally similarities of such contaminations with the products. Contaminations can occur as organic or inorganic materials such as broken or worn part of processing machines; ferromagnetic materials such as iron or steel are routinely removed with strong magnets being also generally useful for paramagnetic contaminants (MESUTRONIC Gerätebau GmbH, 2019); glass or porcelain can be discriminated by their higher density or by vibration spectroscopy (Mekitec, 2022).

Nevertheless, the detection of macromolecular organic contaminants is generally much more difficult because of the similarity to the macromolecular processed food. Currently, there are no methods, which allow an on-site detection and identification of such organic contaminants. A method for the detection of organic contaminant in processed meat like the fluorescence decay time measurement would bring-about an appreciable progress.

The fluorescence decay time can be measured in the time (time-domain fluorimetry) or frequency domain (frequency-domain fluorimetry) (Lakowicz, 2006). The fluorescence decay time, measured in the time domain with a fluorescence spectrophotometer, can be used as an identification feature for plastics (Langhals et al., 2014, 2015). Alternatively, a measurement of the fluorescence decay time can be carried out with an FD-FLIM (frequency-domain fluorescence lifetime imaging microscopy) camera (Chen et al., 2015). It has already been shown that a detection and identification of plastics on soil, at least down to a size of 70 µm is possible (Wohlschläger et al., 2024b). Furthermore, using FD-FLIM in combination with a MLP (Multilayer Perceptron) has proven, that the fluorescence lifetime can be used to identify and discriminate eleven plastic types, tire wear and ten environmental

* Corresponding author.

E-mail address: martin.versen@th-rosenheim.de (M. Versen).

<https://doi.org/10.1016/j.foohum.2024.100363>

Received 10 May 2024; Received in revised form 18 July 2024; Accepted 19 July 2024

Available online 20 July 2024

2949-8244/© 2024 The Authors. Published by Elsevier B.V. This is an open access article under the CC BY license (<http://creativecommons.org/licenses/by/4.0/>).

materials (Wohlschläger et al., 2023; Wohlschläger et al., 2024a, 2024b). At the same time, it was shown that the fluorescence decay time is dependent on the concentration of the dyes in diluted solutions (Langhals & Schlücker, 2022, 2023). These results also give reason to expect that the fluorescence lifetime of a layered structure of different solid matters as salami will change with the composition and the thicknesses of the layers. Thus, we investigate, for example, if four different plastic types can be identified on top, in between and below salami slices, to give a proof of principle that FD-FLIM can be used to directly detect organic contaminants during food production. Additionally, we conducted investigations on the fluorescence bleaching of salami due to prolonged laser exposure.

2. Materials and methods

2.1. Samples

Plastics may be found in processed foodstuff not only from packages and transport vessels and broken parts of engines, but also caused by micro plastics from the environment having reached the food chain. As a consequence, we started first investigations with the detection of the frequently used plastics polyamide (PA), polyethyleneterephthalate (PET) and polyvinylchloride (PVC) on slices of poultry salami prepared and extended to other kinds of salami. Flakes of polymers (1- 2 mm in size) were placed on the surface; these contaminants can be hardly visually detected and distinguished from the fatty component of the poultry salami. For the second investigation, we chose a more application-oriented use-case. In this context, possible source of contamination with plastics in processed foodstuff may be the abrasion or fragmentation of the transport vessels. In Europe, red Euro vessels E2 made from HDPE and mixed with a red colour batch are allowed and used for the transport of meat in factories; as a consequence, fragments of such vessels contaminating the produced meat were studied, preferentially in salami from pork and organic beef. Thus, fragments of about 2 mm diameter were placed above, behind and in between the samples for detection such as between two salami slices. The food samples were stored at 5 °C in a fridge prior to the investigations. To limit any temperature interference, the food samples were taken out of the fridge, prepared with the plastics on glass object holders and directly measured using the described measurement equipment at room temperature of 20 °C and relative humidity of 60 %.

2.2. Measurement equipment

The fluorescence spectrum was measured at 295 nm excitation wavelength and the fluorescence emission spectrum was measured at the maximum of the fluorescence spectra of 333 nm with a Varian Cary Eclipse spectrometer, at a slit width of 2.5 nm. A Laser PhoxX+ 488-100 of Omicron Laserage GmbH with a wavelength of 488 nm and a maximal intensity of 100 mW was applied for the excitation causing fluorescence. Time constants of fluorescence decay were obtained from a 2D matrix of 1008 × 1008 channels by means of a camera pco.film from the Excelitas PCO GmbH. An exact light guidance as well as a mounting for the camera and the laser diode was realized with a microscope, which also is 20 fold enlarging the region of interest. Additionally, three different optical filters were used during the investigations. An optical notch filter was placed in the excitation beam to eliminate any unwanted excitation light. During the preliminary investigations, detecting PA, PET, and PVC on top of and below the salami slices an optical longpass filter was used, i.e., the fluorescence decay behaviour of all emission states was measured. For the application-oriented investigations, detecting HDPE from an Euro vessel E2 on top of, and beneath salami, an optical bandpass filter with a cut-on wavelength of 500 nm and a cut-off wavelength of 550 nm was used, i.e., the fluorescence decay time of each emission state in this wavelength region was measured.

To evaluate the FD-FLIM images, the fluorescence lifetimes in the

images were represented in a histogram of counts n over time t . Afterwards, the fluorescence lifetime histograms were Gaussian analysed ($n = n_0 \cdot \exp(-(t-\tau)^2/(2\sigma^2))$), resulting in the maxima n_0 , the fluorescence lifetimes τ and the standard deviation σ . Since in some cases several maxima were evaluated in the fluorescence spectra and in the fluorescence decay time histograms, the maxima have been numbered consecutively and referenced in the text for a better overview.

3. Results and discussion

3.1. Preliminary investigations

Optical methods for detecting impurities in e.g. processed meat for salami are attractive because of their uncomplicated, reliable and fast operation. However, the intense colour of such optically inhomogeneous products interfere with methods simply using light absorption for detection. Even integrating spheres (Ulbricht bowls) bring about limited improvements because of the remaining light absorption; moreover, some products are stained such as with natural cochineil (carminic acid CAS registry number RN 1260-17-9). On the other hand, processed meat exhibits comparably strong auto fluorescence, which is in accordance to Gatellier et al. (Gatellier et al., 2009); see Fig. 1, 11 for the maximum of the fluorescence excitation spectrum and 12 for the fluorescence spectrum of salami.

Fig. 1 shows the extension of most of the fluorescence in the UV below 400 nm with a weak extension into the visible causing a bluish shining if irradiated with a fluorescent lamp. The adjacent fluorescence excitation spectrum indicates the absorption of the significant chromophores for a fluorescence emission. The fluorescence decays exponentially according to first order where the decay constant can be measured with high precision and is characteristic for the substrate such as a fingerprint, here the investigated salami. On the basis of Fig. 1, one would estimate that an optical excitation at the maximum of the spectrum of fluorescence excitation or at slightly shorter wavelengths would be most appropriate for intense fluorescent signals according to standard procedures in fluorescence spectroscopy, but this would mean an optical excitation in the UV below 300 nm where biological materials are strongly absorbing. As a consequence, the light for optical excitation cannot penetrate deep into the material. Thus, a more bathochromic intense laser line at 488 nm is applied and a sufficiently strong fluorescence signal of all tested samples is obtained; obviously, there are sufficient bathochromically absorbing fluorophores in the samples. All further investigations are concentrated to this wavelength where generally also other wavelengths may be suitable. Since time-domain fluorimetry was used in previous studies, e.g., (Bouchard et al., 2004;

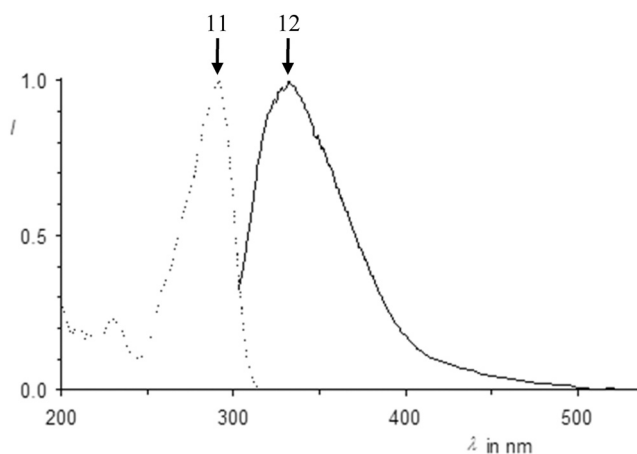


Fig. 1. Fluorescence (right, solid curve, optical excitation at 295 nm) and fluorescence excitation spectrum (left, dotted curve, fluorescence at 333 nm) of commercial salami from mixed pork and beef organic meat.

Bouchard et al., 2006; Langhals et al., 2015) and thus the fluorescence lifetimes of processed meat and plastics at a single emission state were investigated, these measurements are not comparable with those presented here, as the used experimental setup measures the fluorescence lifetime over all emission states.

We started the investigations with salami from turkey with high resolution in time where one observes two maxima of fluorescence decay time statistically scattering around the maxima τ_1 and τ_2 which can be precisely fitted by two Gaussian functions 21 and 22 with the parameters: $\tau_1 = 2.004$ ns, $\sigma_1 = 0.061$ ns, $n_{o1} = 36450$; $\tau_2 = 2.253$ ns, $\sigma_2 = 0.084$ ns, $n_{o2} = 50025$; see Fig. 2. The two Gaussian functions overlay to a single function for lower resolution in time (0.01 ns). If, for economic reasons, all further investigations are carried out with a smaller but more sufficient resolution of 0.01 ns, a global decay time of 2.26 ns can be found.

Further batches concern organic salami from beef 31 ($\tau_1 = 2.60$ ns, $\sigma_1 = 0.09$ ns; $n_{o1} = 34,100$), see Fig. 3, and pork salami 41 ($\tau_1 = 2.33$ ns, $\sigma_1 = 0.093$ ns; $n_{o1} = 34,100$), see Fig. 4. The colour seem to correlate with the time constant of decay because of being slightly prolonged from the rose turkey salami to the red pork salami and further to the dark red beef salami.

A further more important influence is the dependency of the fluorescence lifetime from the light dose of irradiation causing photo bleaching of the fluorophores demonstrated with the poultry salami. The component with longer fluorescence decay becomes more easily bleached than for the shorter decay constant. This causes a shift of the averaged time constant to smaller values depending on the light dose; see Fig. 5.

The photo bleaching can be comparably precisely described according to the first order exponential; see Fig. 5 and the linearization in the inset of Fig. 5. The photo bleaching does not interfere with determination of the time constant for the characterisation of salami because a single dose of irradiation is more than sufficient for such determinations and far away from any photochemical process. On the other hand, this effect may be useful for quality control because generally, the quality of foodstuff declines with the exposure to sunlight. Thus, the shortening of the global time constant of the fluorescence decay can be applied for quality control.

A punctual measurement of the decay time would arbitrarily indicate a contamination of the salami by organic polymers. As a consequence, a larger area was tested by means of a two-dimensional method (2D) where a distribution of time constants of decay was obtained. The auto fluorescence of salami contaminated with the polymers polyamide (PA), polyethyleneterephthalate (PET), polyvinylchloride (PVC) and high density polyethylene (HDPE) was measured in a plane and integrated to

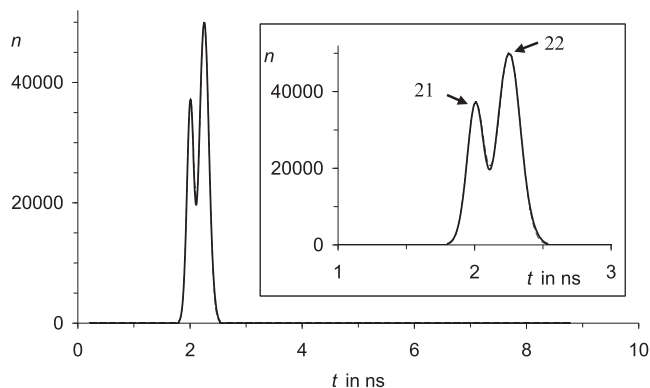


Fig. 2. Fluorescence decay constants of poultry salami optically excited at 488 nm (thick, solid curve); thin, dashed curve (mainly covered by the experimental decay curve); simulated decay characteristic on the basis of a Gaussian analysis. Number n of the photomultiplier counts as a function of the time t. Inset: expanded range between 1 and 3 ns.

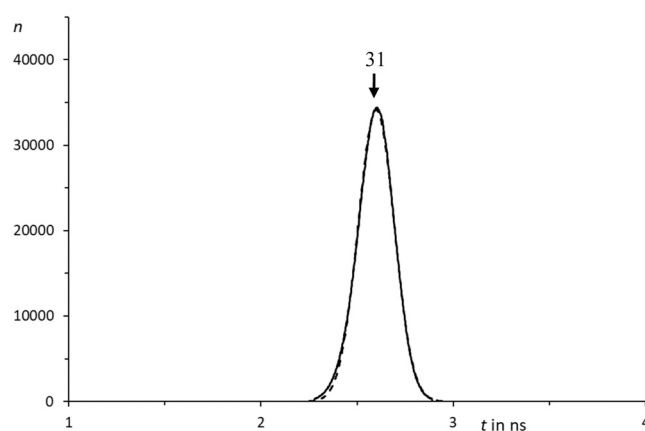


Fig. 3. Fluorescence decay of organic beef salami optically excited at 488 nm (thick, solid curve); thin, dashed curve: simulated decay characteristic on the basis of a Gaussian analysis. Number n of the photomultiplier counts as a function of the time t.

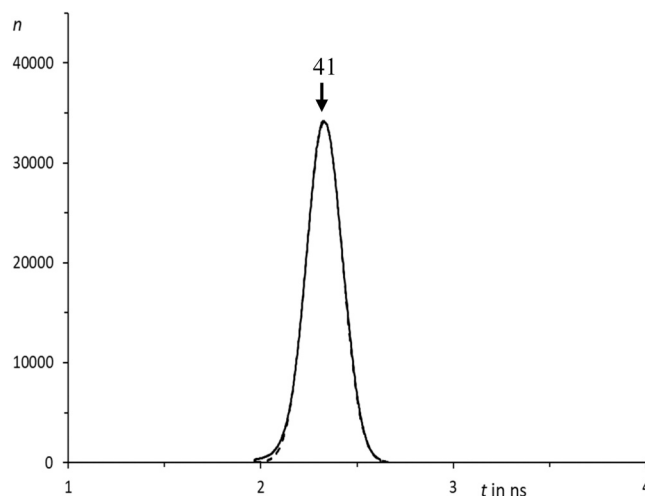


Fig. 4. Fluorescence decay of pork salami optically excited at 488 nm (thick, solid curve); thin, dashed curve: simulated decay characteristic on the basis of a Gaussian analysis. Number n of the photomultiplier counts as a function of the time t.

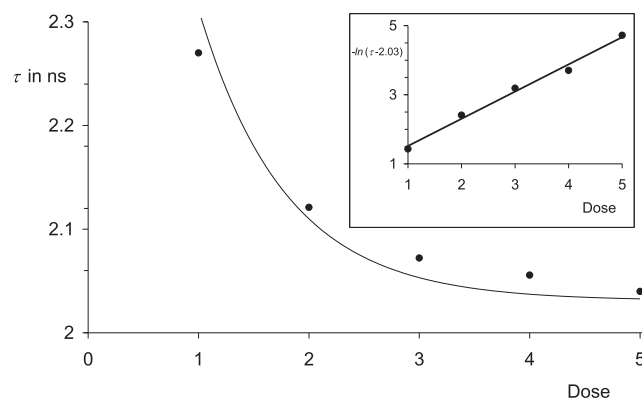


Fig. 5. Dependence of the time constant τ of fluorescence on the light dose of irradiation (points) and approximation according to the first-order (solid curve). Inset: Linearization according to first order; slope 0.788, intercept 0.238; with a χ^2 goodness-of-fit test value of $1.3 \cdot 10^{-4}$ for 5 points.

get a single value for the fluorescence decay.

Firstly, a slice of salami contaminated with hardly visually detectable polyamide gave a distribution of time constants of the auto fluorescence when the plane of a slice was analysed in two dimensions (2D); the components of the obtained constants of decay can be precisely described by Gaussian functions (the experimental values slightly depend on the averaging procedure). We have found a characteristic maximum **64** at $\tau_1 = 2.21$ ns ($\sigma_1 = 0.075$ ns, $n_{o1} = 80,000$) for the salami **61** and a further maximum **66** for the polyamide **63** as the contaminant: $\tau_2 = 3.28$ ns ($\sigma_2 = 0.14$ ns, $n_{o2} = 27,900$); see Fig. 6. Thus, the contamination was unambiguously identified. A third, minor intense maximum **65** at $\tau_3 = 2.91$ ns ($\sigma_2 = 0.27$ ns, $n_{o2} = 20,500$) was detected between the decay times of the salami and the polyamide and is a consequence of the experimental conditions. The time constants of polymer and salami partially overlap at the border **62** where **65** is probably a consequence of the convolution of the fluorescence signal of salami and the polymer.

Salami contaminated at the surface with PVC was analysed in the same way as the results show in Fig. 7. A characteristic maximum **74** at $\tau_1 = 2.62$ ns ($\sigma_1 = 0.12$ ns, $n_{o1} = 172,000$) was found for salami **71** and a further maximum **76** for the contaminating PVC **73**: $\tau_2 = 5.42$ ns ($\sigma_2 = 0.18$ ns, $n_{o2} = 60,000$); thus, the contamination is unambiguously indicated. A third maximum **75** was found at $\tau_3 = 4.38$ ns ($\sigma_2 = 0.18$ ns, $n_{o2} = 18,600$) and is probably a consequence of the overlap of both other signals at the border **72**, which was already observed when PA was under investigation (compare to **65** in Fig. 6).

A contamination of poultry **81** with PET **82** was analysed as a more difficult example because the time constant of decay for meat and PET are more similar than for the other examples; see Fig. 8. Still two maxima were found, **83** for the salami and **84** for the contaminant PET. The result of the Gaussian analysis gave $\tau_1 = 2.33$ ns ($\sigma_1 = 0.074$ ns, $n_{o1} = 250,000$) for **83** and $\tau_2 = 2.50$ ns ($\sigma_2 = 0.069$ ns, $n_{o2} = 19,501$) for **84**. Thus, the method for detection can be successfully applied even when the time constants of fluorescence decay of the sample and the contaminant become more similar.

Moreover, a slice of salami contaminated with polyamide at its lower surface was optically excited through the salami sample; see Fig. 9. Optical conditions become much more complicated because of multiple light scattering and inner filter effects. Nevertheless, the maximum **91** was found where the scattered values could be well-described by a Gaussian function: $\tau = 2.92$ ns ($\sigma = 0.12$ ns, $n_o = 16,950$). A contamination could be detected by the shift of the maximum to longer decay times.

The fluorescence lifetimes of different granular polymer types shown

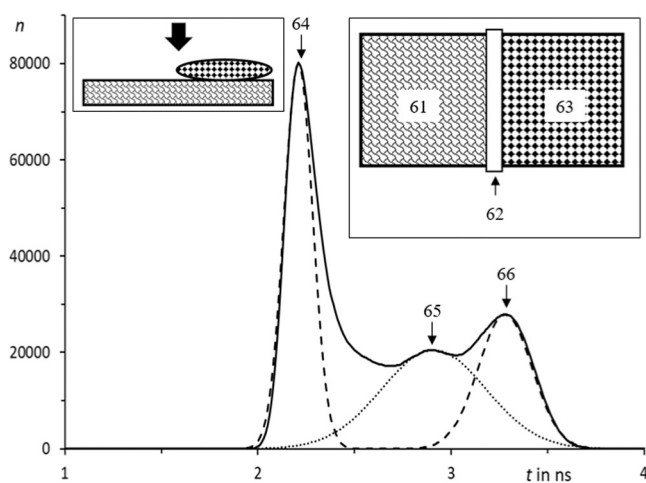


Fig. 6. Fluorescence decay of poultry salami contaminated with PA (excitation at 488 nm). Thick, solid curve: Experimental values, thin, dashed and dotted curves: Simulated values obtained from a Gaussian analysis.

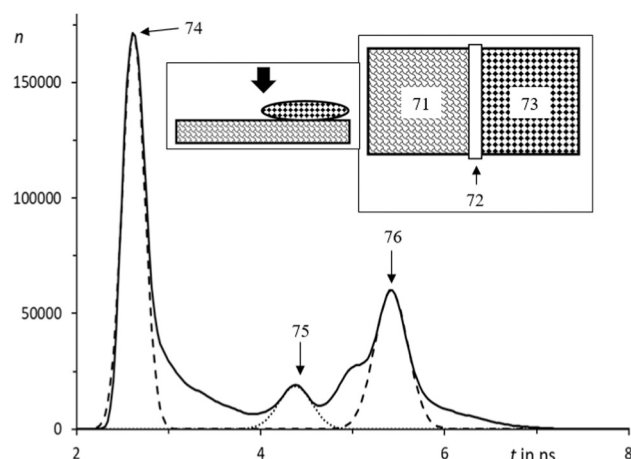


Fig. 7. Fluorescence decay of poultry salami contaminated with PVC (excitation at 488 nm); solid thick curve: Experimental values, thin, dashed curve: Simulated values on the basis of a Gaussian analysis (mostly covered by the experimental curve).

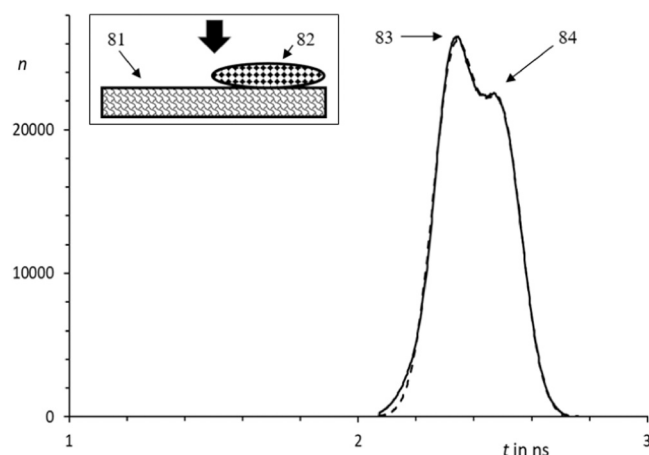


Fig. 8. Fluorescence decay of poultry salami contaminated with PET (excitation at 488 nm); solid thick curve: Experimental values, thin, dashed curve: Simulated values on the basis of a Gaussian analysis (mostly covered by the experimental values).

in (Wohlschläger et al., 2024a) can not be compared to the fluorescence lifetimes of the polymer flakes used in these investigations, as (Langhals et al., 2015) already provided insight that the manufacturing process impacts the decay time. Nevertheless, the fluorescence lifetimes of individually measured flakes of PA, PET, and PVC were reported to $\tau = 4.48$ ns ($\sigma = 0.18$ ns), $\tau = 3.47$ ns ($\sigma = 0.21$ ns), and $\tau = 9.18$ ns ($\sigma = 0.46$ ns), respectively (Wohlschläger et al., 2019). Comparing the individually measured fluorescence lifetimes of the polymers shows that, the polymer types are not directly identifiable due to the mixed fluorescence signals. However, the polymers are detectable due to the shift in fluorescence lifetime.

3.2. Experimental applications

As the results of our preliminary investigations proved that the chosen polymers are detectable on, beneath, and between salami slices, we conducted application-oriented investigations. Here, the aim was to identify red HDPE from an Euro vessel on, beneath, and between salami slices. Worth mentioning is, that ideal polymers without low-lying chromophores such as PE should not show any fluorescence emission. Nevertheless, as the used HDPE is a technical polymer, the

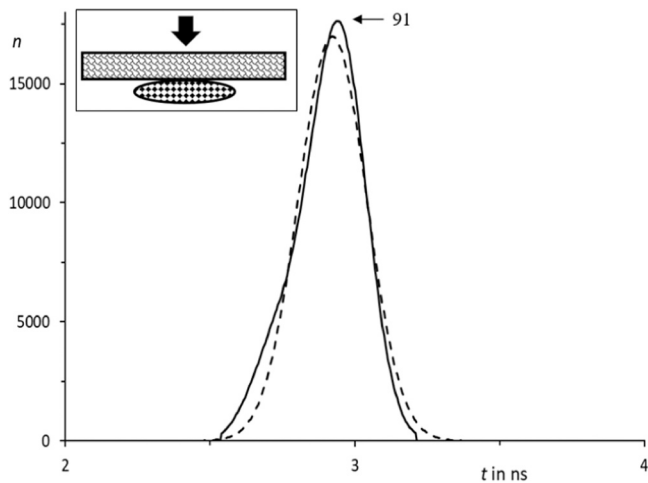


Fig. 9. Fluorescence decay of backward electronically excited poultry salami contaminated with polyamide (excitation at 488 nm); solid thick curve: Experimental values, thin, dashed curve: Simulated values on the basis of a Gaussian analysis (mostly covered by the experimental curve).

manufacturing process causes chain breaks and oxidation products, which may be the reason that fluorescence can be detected. Furthermore, fluorescence can also be caused by additives such as whiteners, UV blockers and thermo-stabilizers which are added to the E2 vessel to improve its durability. Hence, the used E2 vessel should exhibit a measurable fluorescence signal, which was already shown in (Wohlschläger et al., 2024b), where the fluorescence lifetime of the red HDPE was reported as $\tau = 3.52$ ns ($\sigma = 0.21$ ns). The excitation of organic beef salami containing an added fragment of red HDPE gave essentially three maxima of decay time; see Fig. 10. The first constant of decay time **104** $\tau_1 = 2.465$ ns ($\sigma_1 = 0.09$ ns, $n_{o1} = 45,900$) is attributed to the salami **101** itself, the second **105** $\tau_2 = 2.8$ ns ($\sigma_2 = 0.14$ ns, $n_{o2} = 58,000$) to a convolute **102** and the third one **106** $\tau_3 = 3.84$ ns ($\sigma_3 = 0.10$ ns, $n_{o3} = 18,000$) to the HDPE as the material of vessels **103**. The assignment of the third maximum τ_3 to red HDPE can be confirmed by comparison with the fluorescence lifetime of red HDPE reported in (Wohlschläger et al., 2024b). The comparably fewer share of detected photons with a higher fluorescence lifetime of **106** is caused by the small dimensions of the fragment not hindering its detection.

Similar results were obtained for the electronic excitation of the HDPE from the backside through the slice of salami; see Fig. 11. The

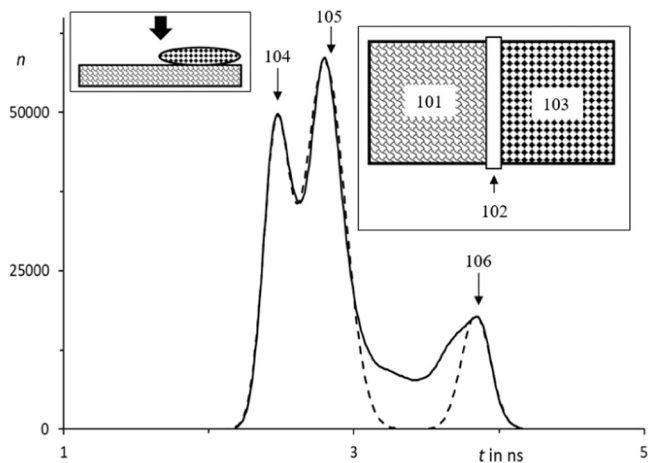


Fig. 10. Fluorescence decay of organic beef salami contaminated with red batched HDPE (electronic excitation at 488 nm); solid thick curve: Experimental values, thin, dashed curve: Simulated values on the basis of a Gaussian analysis (mostly covered by the experimental values).

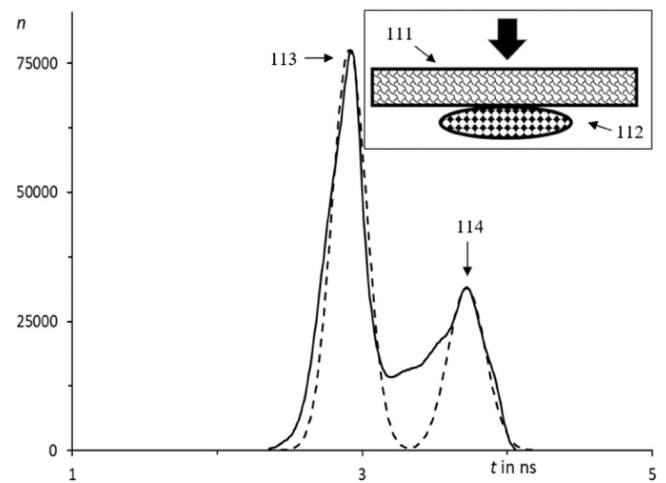


Fig. 11. Fluorescence decay of organic beef salami contaminated with a fragment of red batched HDPE (excitation at 488 nm); solid thick curve: Experimental values for excitation from the backside, dashed curve: Simulated values on the basis of a Gaussian analysis (mostly covered by the experimental values).

characteristic time constant of the salami **111** is lacking; however, a convoluted fluorescence decay time **113** of salami **111** and plastic **112** is observed: $\tau_1 = 2.91$ ns ($\sigma_1 = 0.12$ ns, $n_{o1} = 77,600$) and additionally the time constant **114** of the plastic **112**: $\tau_2 = 3.72$ ns ($\sigma_2 = 0.13$ ns, $n_{o2} = 31,500$) is measured. Here, the assignment of τ_2 to red HDPE is also in accordance to the measured fluorescence lifetime of the material from (Wohlschläger et al., 2024b).

Finally, a fragment of HDPE was placed between two slices of salami. Only mixed fluorescence decay constants were observed in Fig. 12 with a maximum **121** at $\tau_1 = 3.15$ ns ($\sigma_1 = 0.12$ ns, $n_{o1} = 37,450$); this may be a consequence of the even higher fraction of the salami compared with the plastic. However, the contamination can be still detected by the prolongation of the time constant of fluorescence decay. All three examples indicate the possibility of clear discrimination between pure and contaminated salami.

In addition to the investigations with contaminated organic beef salami and poultry salami, the here described method was extended to pork salami and finds its full analogy. Similar results to the beef salami were obtained with a fragment of plastic at the surface; see Fig. 13. A characteristic maximum **134**, for the salami **131** with $\tau_1 = 2.36$ ns ($\sigma_1 =$

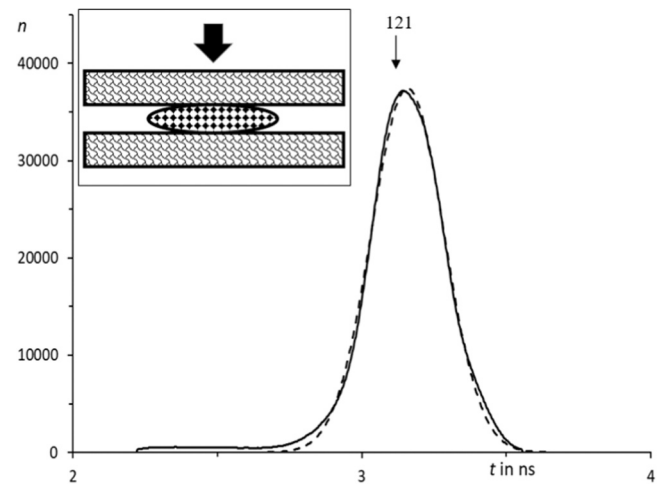


Fig. 12. Fluorescence decay of organic beef salami contaminated with red batched HDPE between two slices (excitation at 488 nm); solid thick curve: experimental values, thin, dashed curve: Simulated values on the basis of a Gaussian analysis (mostly covered by the experimental curve).

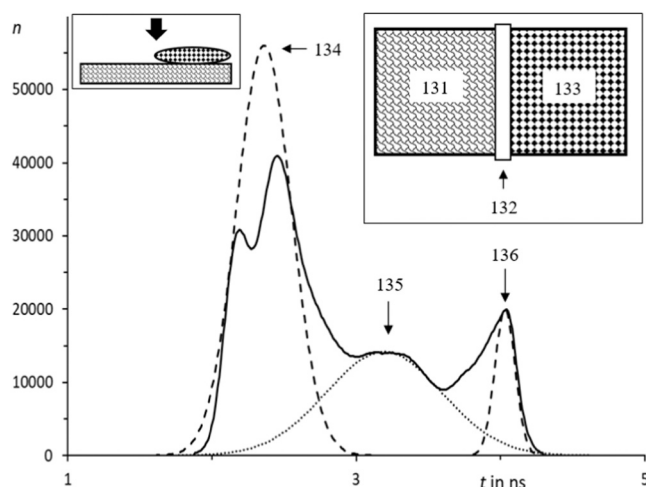


Fig. 13. Fluorescence decay of pork salami contaminated with red batched HDPE (excitation at 488 nm); solid thick curve: experimental values, thin, dashed curve: Simulated values on the basis of a Gaussian analysis (mostly covered by the experimental values).

0.19 ns, $n_{01} = 56,000$), a mixed decay **135** $\tau_2 = 3.2$ ns ($\sigma_2 = 0.40$ ns, $n_{02} = 14,200$) from the convoluted signal of the overlapping region **132**, and the fluorescence **136** of the plastic **133** $\tau_3 = 4.03$ ns ($\sigma_3 = 0.08$ ns, $n_{03} = 20,000$) were obtained. In this context, τ_3 is not directly assignable to HDPE due to convolving fluorescence signals. However, it is reasonable to assume that the fluorescence lifetime can be assigned to HDPE due to its similarity to the reported fluorescence lifetime in (Wohlschläger et al., 2024b).

An excitation of the salami **141** from the backside gave two maxima in Fig. 14. Again, the left maximum **143** is characteristic for the salami **141**: $\tau_1 = 2.44$ ns ($\sigma_1 = 0.14$ ns, $n_{01} = 43,100$) and the right maximum **144** is a mixture of the fluorescence signal of the salami **141** and the plastic **142**: $\tau_2 = 2.73$ ns ($\sigma_2 = 0.065$ ns, $n_{02} = 21,000$).

Finally, a plastic fragment was placed between two slices of the pork salami. The detection is even simpler than with the plastic behind a single slice; see Fig. 15. This may be a consequence of the back scattering of light by the second slice. The decay constant **151** is characteristic for the pork salami: $\tau_1 = 2.485$ ns ($\sigma_1 = 0.19$ ns, $n_{01} = 56,000$); a second maximum **152** is caused by the convolution of the overlapping salami and plastic with $\tau_2 = 3.74$ ns ($\sigma_2 = 0.22$ ns, $n_{02} = 20,600$) and a third decay time which is specific for the red HDPE **153** is: $\tau_3 = 3.98$ ns ($\sigma_3 = 0.066$ ns, $n_{03} = 20,000$). As previously described, τ_3 is not directly assignable to HDPE, but it is reasonable due to its similarity to the reported fluorescence lifetime in (Wohlschläger et al., 2024b).

4. Conclusion

Contaminations of plastics in processed meat such as salami of various sources can be detected by their time constants of fluorescence where the polymers generally exhibit longer time constants of decay than the processed meat. An unambiguous identification of contaminants is even possible if the constants of decay become more similar (PET) or if the contaminant is covered by the tested material.

The short time constants of a few nanoseconds allow very fast rates of processing, where data acquisition is estimated to require about ten time constants and should allow data processing and the recognition of contaminants within the short time of 20 until 100 ns; moreover, the size of the contaminant is of minor importance where grinded plastics and microplastics can be found as well. This is becoming even more important because the exponentially increasing environmental pollution by microplastics is reaching the food chains.

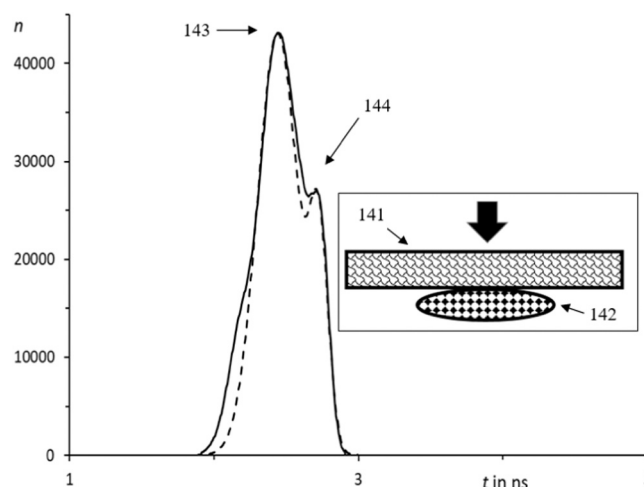


Fig. 14. Fluorescence decay of pork salami contaminated with a fragment of red batched HDPE (excitation at 488 nm); solid thick curve: Experimental curve from backward irradiation, thin, dashed curve: Simulated values on the basis of a Gaussian analysis (mostly covered by the experimental values).

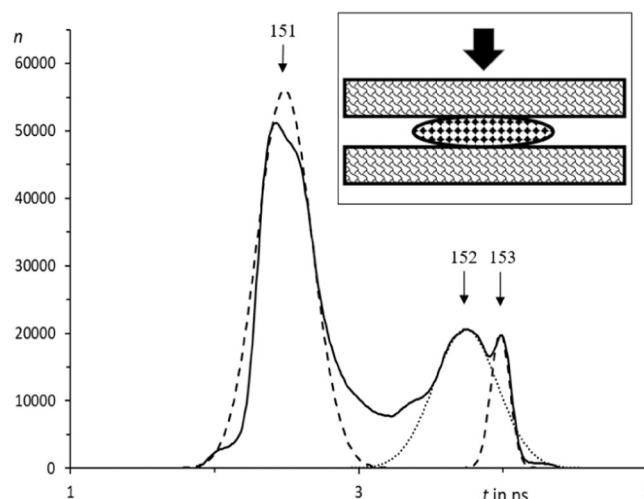


Fig. 15. Fluorescence decay of pork salami contaminated with a fragment of red batched HDPE between two slices of salami (excitation at 488 nm); solid thick curve: experimental curve from backward irradiation, thin, dashed curve: Simulated values on the basis of a Gaussian analysis (mostly covered by the experimental values).

Funding and acknowledgment

Funded by the Deutsche Forschungsgemeinschaft (DFG, German Research Foundation) – Project Number 391977956 – SFB 1357.

CRedit authorship contribution statement

Christian Laforsch: Writing – review & editing. **Martin Versen:** Writing – review & editing, Writing – original draft, Supervision, Investigation. **Maximilian Wohlschläger:** Writing – review & editing, Methodology, Investigation, Formal analysis. **Heinz Langhals:** Writing – review & editing, Methodology, Investigation, Formal analysis.

Declaration of Competing Interest

The authors declare that they have no known competing interests (not limited to financial aspects) or personal relationships that could have appeared to influence the work reported in this paper.

References

- Bouchard, A., Fréchette, J., Long, W. F., Vernon, M., Cormier, J.-F [Jean-François], Vallée, R., Mafu, A. A [Akier A.], & Lemay, M.-J. (2004). Non-contact characterization of bacteria by time-resolved fluorescence. In A. Mahadevan-Jansen, M. G. Sowa, G. J. Puppels, Z. Gryczynski, T. Vo-Dinh, & J. R. Lakowicz (Eds.), *SPIE Proceedings, Biomedical Vibrational Spectroscopy and Biohazard Detection Technologies* (p. 250). SPIE. <https://doi.org/10.1117/12.526613>.
- Bouchard, A., Fréchette, J., Vernon, M., Cormier, J.-F [Jean-François], Beaulieu, R., Vallée, R., Mafu, & A. A [Akier Assanta]. (2006). Optical characterization of *Pseudomonas fluorescens* on meat surfaces using time-resolved fluorescence. *Journal of Biomedical Optics*, 11(1), 14011. <https://doi.org/10.1117/1.2162166>.
- Chen, H., Holst, G., & Gratton, E. (2015). Modulated CMOS camera for fluorescence lifetime microscopy. *Microscopy Research and Technique*, 78(12), 1075–1081. <https://doi.org/10.1002/jemt.22587>
- DIN Deutsches Institut für Normung e. V. (12.1994). *Transportkette für Fleisch und Fleischerzeugnisse – Teil 1: Starre, stapelbare Mehrwegtransport- und Lagerkästen aus Kunststoff; Maße, Gewichte, Ausführung* (DIN Norm). Beuth Verlag GmbH.
- Gatellier, P., Santé-Lhoutellier, V., Portanguen, S., & Kondjoyan, A. (2009). Use of meat fluorescence emission as a marker of oxidation promoted by cooking. *Meat Science*, 83(4), 651–656. <https://doi.org/10.1016/j.meatsci.2009.07.015>
- Lakowicz, J. R. (2006). *Principles of fluorescence spectroscopy (3rd ed) (3rd ed.)*. Springer.
- Langhals, H., & Schlücker, T. (2022). Dependence of the Fluorescent Lifetime τ on the Concentration at High Dilution. *The Journal of Physical Chemistry Letters*, 13(32), 7568–7573. <https://doi.org/10.1021/acs.jpcllett.2c01447>
- Langhals, H., & Schlücker, T. (2023). Reply to "Comment on 'Dependence of the Fluorescent Lifetime τ on the Concentration at High Dilution'": Extended interpretation. *The Journal of Physical Chemistry Letters*, 14(6), 1457–1459. <https://doi.org/10.1021/acs.jpcllett.3c00038>
- Langhals, H., Zgela, D., & Schlücker, T. (2014). High performance recycling of polymers by means of their fluorescence lifetimes. *Greening and Sustainable Chemistry*, 04(03), 144–150. <https://doi.org/10.4236/gsc.2014.43019>
- Langhals, H., Zgela, D., & Schlücker, T. (2015). Improved high performance recycling of polymers by means of bi-exponential analysis of their fluorescence lifetimes. *Greening and Sustainable Chemistry*, 05(02), 92–100. <https://doi.org/10.4236/gsc.2015.52012>
- Mekitec. (2022). *Improving Glass Detection: In Food Production*. (<https://www.mekitec.com/glass-detection-in-food/>).
- MESUTRONIC Gerätebau GmbH. (2019). *METALLENDETEKTOREN UND -SEPARATOREN: FÜR DIE FLEISCHVERARBEITENDE INDUSTRIE*. (https://www.mesutronic.de/wp-content/uploads/2019/01/D-Mesutronic_Fleischprospekt_20181121-web.pdf).
- Wohlschläger, M., Leiter, N., Dietlmeier, M., Löder, M. G., Versen, M., & Laforsch, C. (2023). Comparison of Two Classification Methods Trained with FD-FLIM Data to Identify and Distinguish Plastics from Environmental Materials. *2023 International Joint Conference on Neural Networks (IJCNN)* (pp. 1–9). IEEE., <https://doi.org/10.1109/IJCNN54540.2023.10191054>
- Wohlschläger, M., Versen, M., Holst, G., & Franke, R. (2019). An Approach of Identifying Polymers With Fluorescence Lifetime Imaging. October 17–18. *2019 IEEE International Conference on Electrical Engineering and Photonics (EExPolytech)* (pp. 186–189). IEEE., <https://doi.org/10.1109/EExPolytech.2019.8906800>. October 17–18.
- Wohlschläger, M., Versen, M., Löder, M. G. J., & Laforsch, C. (2024a). Identification of different plastic types and natural materials from terrestrial environments using fluorescence lifetime imaging microscopy. *Analytical and Bioanalytical Chemistry*, 416(15), 3543–3554. <https://doi.org/10.1007/s00216-024-05305-w>
- Wohlschläger, M., Versen, M., Löder, M. G. J., & Laforsch, C. (2024b). A promising method for fast identification of microplastic particles in environmental samples: A pilot study using fluorescence lifetime imaging microscopy. *Heliyon*, 10(3), Article e25133. <https://doi.org/10.1016/j.heliyon.2024.e25133>